

Al₂O₃ coatings against high temperature corrosion deposited by metal–organic low pressure chemical vapour deposition

H. D. van Corbach, V. A. C. Haanappel, T. Fransen* and P. J. Gellings

University of Twente, Department of Chemical Technology, P.O. Box 217, 7500 AE Enschede (Netherlands)

(Received July 1, 1993; accepted September 8, 1993)

Abstract

Metal–organic chemical vapour deposition of thin amorphous films of Al₂O₃ on steels was performed at low pressure. Aluminium tri-sec-butoxide (ATSB) was used as a precursor. The effects of the deposition temperature (200–380 °C), the deposition pressure (0.17–1.20 kPa) and the ATSB concentration ((5.5–33.5) × 10⁻⁴ kPa) were studied with respect to the growth rate of the coating and the sulphidation properties at high temperatures. The sulphidation experiments were performed for 70 h at 450 °C in a gas atmosphere consisting of 1% H₂S, 1.5% H₂O, 19% H₂, Ar balance. From the results and scanning electron microscopy observations the best process conditions were determined.

1. Introduction

Metal–organic chemical vapour deposition (MOCVD) of thin amorphous films of Al₂O₃ for use in electronic devices has been reported by several authors [1–3]. In recent years Al₂O₃ has also been investigated for application as a protective coating against high temperature corrosion in coal gasification environments. The Al₂O₃ coatings were produced by MOCVD using the metal alkoxides aluminium tri-isopropoxide (Al(OC₃H₇)₃) [4] and aluminium tri-sec-butoxide (ATSB) (Al(OC₄H₉)₃) [3, 5, 6] as precursors. The application of metal alkoxides as precursors has several advantages: (1) these compounds can be purified to a high degree; (2) they contain enough oxygen for the formation of the desired oxide, which means that no additional compounds have to be added to the gas stream—this is an advantage over the use of trimethyl aluminium (TMA) with oxygen or nitrous oxide [7]; (3) the deposition temperature is much lower than for the formation of Al₂O₃ from AlCl₃, CO₂ and H₂ [8, 9].

ATSB has until recently been used only as a precursor for the deposition of Al₂O₃ at atmospheric pressure [5, 6]. From the results obtained it was clear that more research was necessary to produce crack- and pore-free Al₂O₃ coatings. Besides modification of the process by adding various substances to the reaction gas mixture [9, 10] or thermal annealing [11, 12], another option is to reduce the total system pressure. Generally, reduced

pressures enhance the diffusivity of the vapour species, with better mixing of the process gas [10, 13].

The aim of this study was to produce crack- and pore-free coatings. Experiments were performed to determine the optimum deposition conditions for an Al₂O₃ coating at low pressures using ATSB as the precursor. This paper reports the deposition kinetics of Al₂O₃ on AISI 304 at various deposition temperatures, reactor pressures and ATSB partial pressures. Sulphidation experiments were performed to determine the protectiveness of the Al₂O₃ coated specimens against high temperature corrosion. From these results and SEM observations the optimum deposition conditions regarding the corrosion resistance of the Al₂O₃ coating were obtained.

2. Experimental details

The Al₂O₃ coatings were deposited by pyrolysis of ATSB (Janssen Chimica) in a low pressure chemical vapour deposition (LPCVD) system, schematically depicted in Fig. 1. The system consisted of a horizontal quartz tube reactor (134 cm long, 10 cm in diameter) in a three-zone furnace (Tempress model Omega Junior). The specimens were attached to a 30 cm glass rod (eight specimens of 12 mm diameter, 3 cm apart; or four specimens of 20 mm diameter, 6 cm apart) parallel to the gas stream. The glass rod was placed 30 cm from the entrance of the tube. A stream of pure nitrogen gas (Praxair nitrogen 5.0) passed through the ATSB precursor in a silicon oil bath. ATSB is a slightly yellow clear,

*Author to whom correspondence should be addressed.

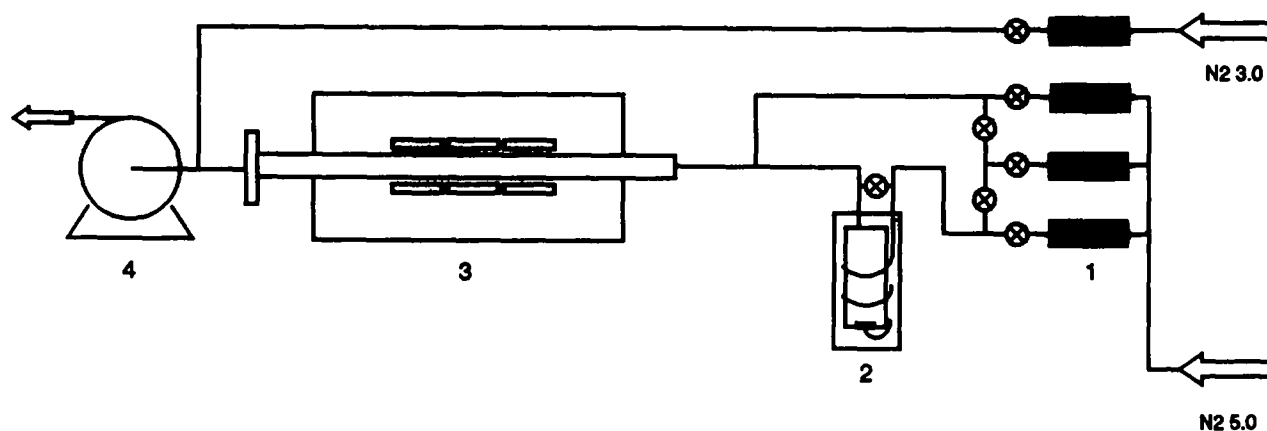


Fig. 1. Schematic view of the MOLPCVD reactor: (1) mass flow controllers; (2) container with ATSB at constant temperature; (3) three-zone furnace; (4) vacuum pump.

moisture- and air-sensitive liquid and has a vapour pressure of 0.133 kPa (1 Torr) at 138 °C. This saturated gas was then diluted with pure nitrogen gas before entering the reactor. The gas line between the ATSB container and the reactor was heated to 150 °C to prevent condensation of the precursor. All gas streams were controlled by electronic mass flow controllers (Brooks 5850TR). The deposition temperature was monitored by three thermocouples which extended into the reactor below the specimens. The temperature profile was maintained as constant as possible (± 0.5 °C) over the length of the specimen load. The reactor pressure during deposition was monitored by capacitive pressure sensors (MKS Baratron type 122A) and kept at the desired value by adding an excess flow of nitrogen to the vacuum pump (Leybold D65BCS).

The typical procedure for an LPCVD experiment was: (1) adjust the reactor temperature to the desired value; (2) load the specimens; (3) open all valves; (4) evacuate the reactor and adjust the flow rates of the dilution gas, the ATSB-containing gas and the excess flow to the vacuum pump; (5) when the temperature of the three zones is within 1 °C of the desired value, start the deposition by closing the valve in the bypass above the ATSB container (Fig. 1); (6) stop the deposition by opening the bypass valve and disconnecting the pump from the system.

Deposition experiments were performed on the alloy AISI 304 (18%–20% Cr, 8%–12% Ni, 0.08% C, 1% Si, 2% Mn, Fe balance). The discs were cut from an electropolished metal sheet and ultrasonically cleaned for 30 min, then further cleaned with soap (Fluka RBS solid), hexane and ethanol. Finally the samples were immersed in Struer's etching fluid (5% solution of 3 M nitric acid in ethanol) for 15 min, washed with ethanol (p.a. grade) and dried with hot air.

The growth rate of the coatings was determined by weighing the samples before and after the deposition

process. The coatings were characterized by sulphidation for 70 h at 450 °C in a gas mixture of composition 1% H_2S , 1.5% H_2O , 19% H_2 , Ar balance. After completion of the sulphidation, the samples were weighed and analyzed by means of a scanning electron microscope (Jeol 35-CF) with an EDX analyzer (KEVEX Delta Class III).

3. Results and discussion

3.1. Deposition experiments

The major difference between the atmospheric and the low pressure chemical vapour deposition is the enhancement of the mass flux of gaseous reactants and products through the stagnant boundary layer between the gas bulk phase and the specimen surface. For the deposition of coatings with uniform thickness, it is necessary to perform the MOCVD process under reaction rate-limited conditions. To quantify the regions of rate and diffusion limitation, experiments were performed to determine the deposition rate as a function of the deposition temperature. Initially, the most suitable conditions considering the gas composition had to be determined. In this first stage the most important variables were the ATSB partial pressure and the total gas flow through the reactor. From Morssinkhof's [4] and our own results, a precursor partial pressure between 5.5×10^{-4} kPa and 33.5×10^{-4} kPa and a deposition temperature of 300 °C (metal-organic LPCVD (MOLPCVD)) were most promising. At higher ATSB partial pressures the coatings were covered with a small amount of powder. This indicated that the products, from a homogeneous reaction of ATSB to Al_2O_3 in the gas phase, partly deposited on the specimen surface. When using lower ATSB partial pressures it was more difficult to obtain a homogeneous and uniform coating: the bulk concentration of ATSB in the gas phase was

TABLE 1. Experimental details

Gas flow rate	11 min ⁻¹
Partial pressure ATSB	(5.6–33.5) × 10 ⁻⁴ kPa
Furnace temperature	200–380 °C
Saturation temperature ATSB	112–138 °C
Reactor pressure	0.17–1.20 kPa

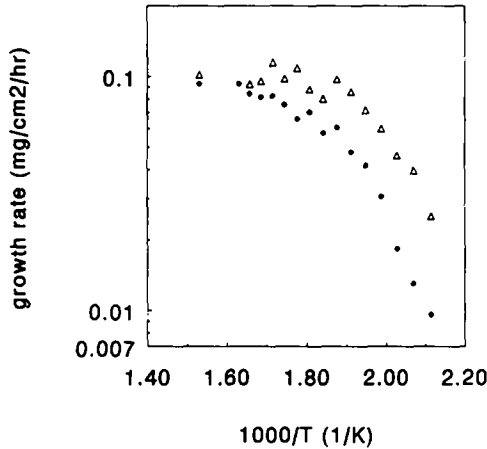


Fig. 2. Arrhenius plot Al₂O₃ deposition on 12 mm diameter AISI 304, $P_{\text{ATSB}} = 7.5 \times 10^{-4}$ kPa, $P_{\text{reactor}} = 0.17$ kPa and 0.40 kPa: ●, 0.17 kPa; ▲, 0.40 kPa.

probably too low. The total gas flow was 11 min⁻¹ (standard temperature and pressure). The range of experimental conditions used is given in Table 1.

Figure 2 shows the Arrhenius plot of the deposition of Al₂O₃ on AISI 304 (diameter 12 mm). The growth rate of the coatings increases with increasing temperature, but from temperatures of around 290–300 °C and higher the growth rate increases much more slowly. This is explained by a change from reaction rate- to diffusion rate-limited growth. Within the region of reaction rate control, the growth rates of the coatings have an almost constant value along the glass rod, but at higher temperatures the deposition rates scatter. The slopes of the plots in the reaction rate limitation regime were calculated to be 65 ± 2 kJ mol⁻¹. This value is lower than the one obtained from atmospheric pressure CVD (83 ± 5 kJ mol⁻¹) [6]. Furthermore, the growth rates are about 10 times lower at 0.17 kPa and the coatings have less variations in colour, so they are more uniform.

The diffusion rate of the reactants in the vapour increases when the total pressure in the reactor decreases. A simplified equation for the reaction rate can be derived [14]

$$\text{reaction rate} = \frac{[A]_{\text{r, bulk}}}{\frac{1}{k_{\text{g}}} + \frac{1}{k_{\text{r}}}} \quad (1)$$

where $[A]_{\text{r, bulk}}$ is the partial pressure of ATSB in the bulk phase, k_{g} is the mass transfer coefficient in the gas phase and k_{r} is the heterogeneous reaction rate constant. The mass transfer coefficient is equal to the ratio between the diffusion coefficient D of the reactive species in the gas phase and the thickness δ of the boundary layer; the heterogeneous reaction rate constant can be calculated from the well known Arrhenius equation.

Kinetic theory predicts that the diffusivity D depends on pressure and temperature [13]

$$D = D_0 \frac{P_0}{P} \left(\frac{T}{T_0} \right)^n \quad (2)$$

where n is 1.8, D_0 is the value of D measured at standard temperature and pressure, P_0 is the standard pressure (99 kPa) and T_0 is the standard temperature (273 K). When T is constant, D varies inversely with pressure.

The thickness δ of the boundary layer at a position X on the substrate [10] is given by

$$\delta = a \left(\frac{\mu X}{\rho v} \right)^{1/2} \quad (3)$$

where a is a proportionality constant, μ is the dynamic viscosity of the gas, v is the velocity of the gas and ρ is the density of the gas. It is assumed that the viscosity is independent of the pressure; and the velocity, at constant temperature, varies inversely proportionally with pressure whereas the density of the gas varies directly proportionally with pressure. From this it can be concluded that at a constant temperature and gas flow (STP) δ is independent of the system pressure when the same experimental set-up is used. Table 2 shows the process parameters (based on data from ref. 14) calculated for 300 °C (deposition temperature) and for 0.17 kPa and 99 kPa reactor pressure. For the two process parameters the gas velocities are obtained with different experimental set-ups, so in this case the product of v and ρ is not constant. From Table 2 it is clear the mass transfer coefficient k_{g} is roughly 100 times higher in the case of low pressure depositions than for atmo-

TABLE 2. Overview of MOCVD process parameters at 300 °C

	$P = 0.17$ kPa (1.25 Torr)	$P = 99$ kPa (760 Torr)	Units
D	1.9×10^{-2}	3.0×10^{-5}	m ² s ⁻¹
v	2.7	0.14 ^a	m s ⁻¹
μ	2.6×10^{-5}	2.6×10^{-5}	kg m ⁻¹ s ⁻¹
ρ	9.8×10^{-4}	0.60	kg m ⁻³
$\delta(X = 0.005 \text{ m})$	7.0×10^{-3}	1.2×10^{-3}	m
$k_{\text{g}} (= D/\delta)$	2.7	2.5×10^{-2}	m s ⁻¹

^aRef. 14.

spheric depositions. This will generally result in improved thickness uniformity, fewer pores and better step coverage [13]. When the mass transfer coefficient increases, the critical temperature range where the deposition mechanism changes from reaction rate to diffusion rate limitation will increase, considering that the heterogeneous reaction rate constant does not change with the partial pressure of ATSB. This means that uniform coatings can be deposited at higher deposition temperatures. In our case the slopes of the plots were $65 \pm 2 \text{ kJ mol}^{-1}$ at low and $83 \pm 5 \text{ kJ mol}^{-1}$ [6] at atmospheric pressure. But a shift of the critical temperature to a lower value (from 370°C (atmospheric pressure) to 300°C (low pressure)) was observed. This might be explained by a change in the Langmuir–Hinshelwood mechanism, resulting in a variation of the heterogeneous reaction rate constant. The more uniform coating might be explained by the increase of k_g . The lower growth rate can be explained by the lower ATSB partial pressures used or a different reaction mechanism, but a detailed description is not yet available.

The major advantage of low pressure depositions is the more uniform coating thickness over a large temperature range, obtained in a large reactor zone with a constant growth rate. Each point plotted in Fig. 2 represents the mean value of the growth rates of the eight samples along the glass rod. It also shows that the difference in growth rate between the two deposition pressure decreases with increasing temperature. Since the diffusivity of the vapour species increases with decreasing pressure, depositions performed at 0.17 kPa in the reaction rate-limited temperature region with almost similar growth rates should result in a better area coverage than the 0.40 kPa depositions.

To investigate the influence of the sample size on the deposition kinetics, an Arrhenius plot was made using AISI 304 specimens of 20 mm diameter at a reactor pressure of 0.17 kPa . Figure 3 shows that the growth rate is not constant along the glass rod at high and low deposition temperatures, but only between 250°C and 290°C . The growth rate of 20 mm diameter specimens is slightly lower than that of the 12 mm samples.

Figure 4 shows the growth rate of Al_2O_3 for a range of reactor pressures. With increasing pressure, up to about 0.93 kPa , the growth rate increases; it is constant at 1.20 kPa . This is probably due to the depletion of the reactant by a homogeneous reaction in the gas phase, where less reactant is available for the heterogeneous reaction on the substrate. The occurrence of a homogeneous reaction was clearly visible as a haze of white powder on the specimens. From eqn. (2) it can be calculated that the diffusivity decreases linearly with increasing pressure, which means that at 0.93 kPa D is 5.6 times smaller than 0.17 kPa . The mean distance

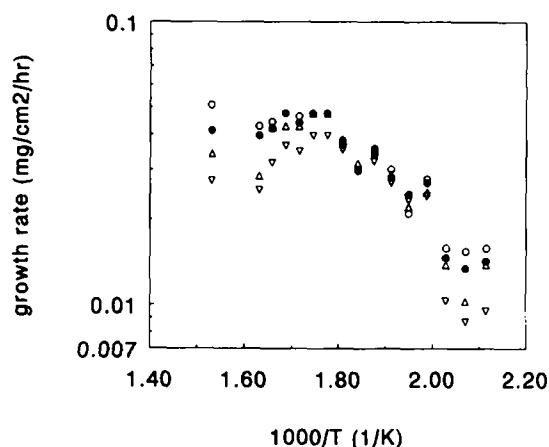


Fig. 3. Arrhenius plot Al_2O_3 deposition on 20 mm diameter AISI 304, $P_{\text{ATSB}} = 7.5 \times 10^{-4} \text{ kPa}$, $P_{\text{reactor}} = 0.17 \text{ kPa}$; positions A, B, C, D are 30 cm (∇), 36 cm (\triangle), 42 cm (\bullet) and 48 cm (\circ) from the reactor entrance respectively.

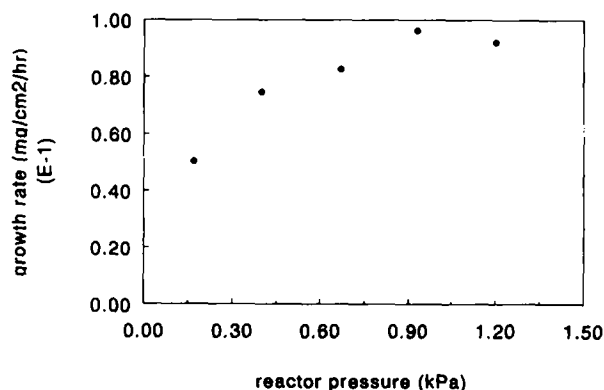


Fig. 4. Growth rate ($\text{mg cm}^{-2} \text{ h}^{-1}$) as a function of total reactor pressure (kPa); $T = 270^\circ\text{C}$, $P_{\text{ATSB}} = 9.3 \times 10^{-4} \text{ kPa}$.

traveled by molecules between successive collisions, called the mean free path λ_{mfp} , is an important parameter of gases and depends on the pressure [13], following

$$\lambda_{\text{mfp}} = \frac{5 \times 10^{-3}}{P} \quad (4)$$

with λ_{mfp} in cm and P in torr. A rise in system pressure will lead to a decline of the mean free path and a rise of the number of collisions per second. From the fact that (for experiments performed in the reaction rate-limited regime) the diffusion coefficient decreases but the growth rate at first increases, it might be concluded that at low pressures the reaction of ATSB to Al_2O_3 is collision activated. At pressures of 0.17 , 0.40 and 0.67 kPa the diffusivity and mean free path are large enough to let more reactive molecules reach the substrate with increasing pressure. At 1.20 kPa the mean free path and the diffusivity have such a low value that the homogeneous reaction rate will increase. Another

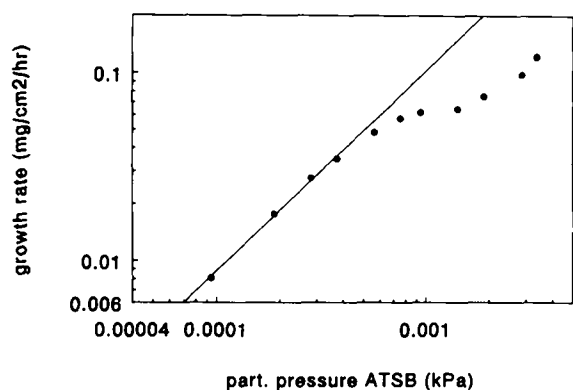


Fig. 5. Reaction order plot for growth rate ($\text{mg cm}^{-2} \text{h}^{-1}$) as a function of ATSB partial pressure (kPa); $T = 270^\circ\text{C}$, $P_{\text{reactor}} = 0.17 \text{ kPa}$.

possibility is that there are no additional free adsorption sites available on the substrate, resulting in a stabilization of the film growth. The homogeneous reaction can be performed by several mechanisms, such as, consecutively, collision activation and nucleation, or pyrolytic decomposition and nucleation.

The order of the reaction with respect to ATSB was determined at a deposition temperature of 270°C and a total pressure of 0.17 kPa (Fig. 5). The slope of the line in Fig. 5 is 1.0. The slope decreases with increasing ATSB partial pressure, reaching a value of zero and then increasing. On the samples representing the last three points of the graph a considerable amount of powder was present. Since the diffusion coefficient and the mean free path of the reactive molecules hardly change with increasing ATSB vapour pressure, the stabilization in growth rate must be due to the increase of the homogeneous reaction, with the normal deposition of Al_2O_3 on the substrate still taking place. When the ATSB partial pressure is increased to a value where the slope of the plot is zero, there is probably a diffusion limitation of reactive molecules, while with a further rise in ATSB partial pressure Al_2O_3 powder, from the homogeneous reaction, will deposit on the specimen causing the rise in experimental growth rate.

3.2. Sulphidation experiments

The sulphidation resistance of the obtained coatings was investigated in the corrosive gas mixture at 450°C for 70 h. The coated samples ($\pm 0.5 \mu\text{m } Al_2O_3$) were compared with an uncoated specimen that was exposed in the same tube. Figure 6 shows the relative sulphidation of 12 mm diameter samples deposited at 0.17 kPa and 0.40 kPa total pressure, and 20 mm diameter samples deposited at 0.17 kPa . The weight gain due to sulphidation of both 0.17 kPa deposited specimen ranges decreases with increasing deposition temperature until 280°C , and increases with a further rise in temper-

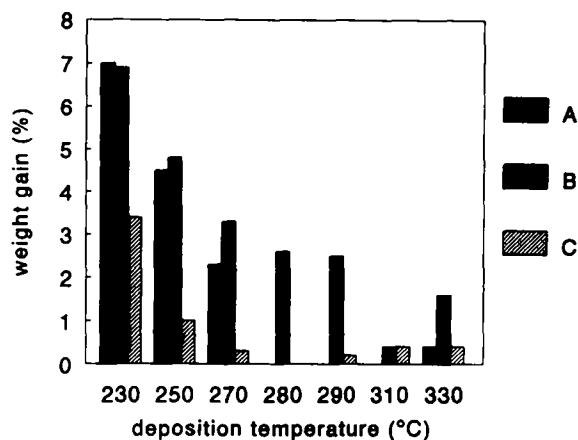


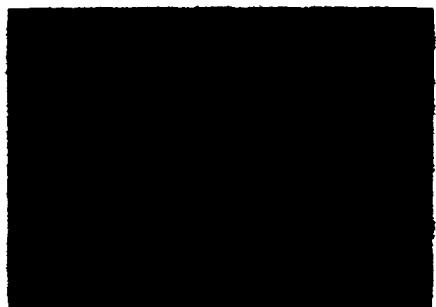
Fig. 6. Comparison of relative weight gain after sulphidation at 450°C for 70 h (uncoated sample = 100%); (A) 12 mm diameter, $P_{\text{reactor}} = 0.17 \text{ kPa}$; (B) 12 mm diameter, $P_{\text{reactor}} = 0.40 \text{ kPa}$; (C) 20 mm diameter, $P_{\text{reactor}} = 0.17 \text{ kPa}$.

ature. The 0.40 kPa deposited specimens have a maximum sulphidation resistance at 310°C , but the protection by the coating is worse than that of the 0.17 kPa deposited specimens. Furthermore, it is clear that the relative weight gain of the 20 mm diameter samples is generally less than that of the 12 mm diameter samples. The weight gain of some samples was zero; no bars are shown in Fig. 6 for these. From SEM observations it was clear that at a deposition temperature of $200\text{--}270^\circ\text{C}$ the amount of cracks in the coating decreased with increasing temperature. Figure 7(a) shows an example of a coating after sulphidation, deposited at 260°C . At 280°C (Fig. 7(b)) the coating on the 20 mm diameter sample was completely free of cracks. With a further increase in temperature (Fig. 7(c), at 310°C), small pores appeared on the surface which increased in number with increasing deposition temperature. The sulphidation product in both cracks and pores was FeS . Specimens deposited at 0.40 kPa were never free of cracks or pores, so that from these observations 0.17 kPa seems to be the best deposition pressure.

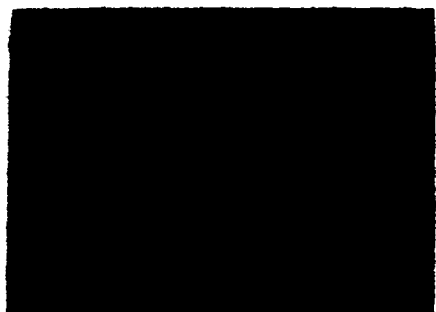
Figure 8 shows the dependence of the ATSB partial pressure on the relative weight gain by sulphidation as compared to an uncoated sample. The deposition temperature was chosen as 270°C , because at this temperature a large range of ATSB partial pressures was applicable without powder deposition on the specimens. The best results were obtained using an ATSB partial pressure of $7.5 \times 10^{-4} \text{ kPa}$. SEM analysis revealed that higher and lower partial pressures resulted in cracked coatings. Similarly, a deposition temperature of 280°C and an ATSB partial pressure of $9.3 \times 10^{-4} \text{ kPa}$ produced the best protecting Al_2O_3 coatings, no relative weight gain and no pores and cracks.



(a)



(b)



(c)

Fig. 7. SEM image of the surface of a coated sample after 70 h of sulphidation at 450 °C; (a) T deposition = 260 °C; (b) T deposition = 280 °C; (c) T deposition = 310 °C.

4. Conclusions

Al_2O_3 coatings were produced on the alloy AISI 304 by MOLPCVD using ATSB as the precursor. The experimental activation energy of this reaction is $65 \pm 2 \text{ kJ mol}^{-1}$. At low ATSB partial pressures the order of the reaction with respect to ATSB is 1.0. Sulphidation experiments showed that the best protecting Al_2O_3 coatings with uniform thickness and without cracks and pores are obtained under the following conditions: gas flow rate 1 l min^{-1} (2.7 m s^{-1}); ATSB

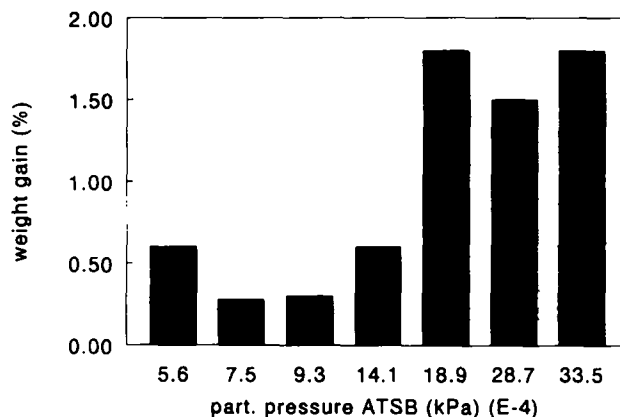


Fig. 8. Relative weight gain of Fig. 5 specimens, sulphidation at 450 °C for 70 h (uncoated sample = 100%).

partial pressure $9.3 \times 10^{-4} \text{ kPa}$; furnace temperature 280 °C; ATSB saturation temperature 138 °C, reactor pressure 0.17 kPa.

Acknowledgments

This research was supported by the Innovative Research Program on Technical Ceramics (IOP-TK) with financial aid of the Dutch Ministry of Economic Affairs.

References

- 1 J. Saraie, J. Kwon, and Y. Yodogawa, *J. Electrochem. Soc.*, **132** (1985) 890.
- 2 A. A. Barybin and V. I. Tomilin, *Zh. Prikl. Khim.*, **49** (1976) 1699.
- 3 J. A. Aboaf, *J. Electrochem. Soc.*, **114** (1967) 948.
- 4 R. W. J. Morssinkhof, *Thesis*, University of Twente, Enschede, 1991.
- 5 V. A. C. Haanappel, H. D. van Corbach, T. Fransen and P. J. Gellings, *Mater. Sci. Eng. A*, **167** (1993) 179.
- 6 V. A. C. Haanappel, H. D. van Corbach, T. Fransen and P. J. Gellings, *Thin Solid Films*, **230** (1993) 138.
- 7 K. Gustin and R. G. Gordon, *J. Electron. Mater.*, **17** (1988) 509.
- 8 P. Wong and M. Robinson, *J. Am. Ceram. Soc.*, **53** (1970) 617.
- 9 H. Altena, G. Pauer, P. Wilhartiz and B. Lux, in J.-O. Carlsson and J. Lindstroem (eds.), *Proc. 5th European Conf. on Chemical Vapour Deposition*, Uppsala, Sweden, 1985, Dept. Chem., Uppsala University, Sweden, 1985, p. 334.
- 10 J.-O. Carlsson, *Thin Solid Films*, **130** (1985) 261.
- 11 S. B. Desu, *J. Am. Ceram. Soc.*, **72** (1989) 1615.
- 12 S. B. Desu, *Jpn. J. Appl. Phys.*, **30** (1991) L2123.
- 13 M. Ohring, *The Materials Science of Thin Films*, Academic, San Diego, CA, 1992.
- 14 V. A. C. Haanappel, H. D. van Corbach, T. Fransen, and P. J. Gellings, *High Temp. Mater. Processes*, in press.